34th Annual International Conference of the IEEE EMBS
San Diego, California USA, 28 August - 1 September, 2012

Quantification of spontaneous and evoked HFO's in SEEG recordings and prospective for pre-surgical diagnostics. Case study.*

Stiliyan Kalitzin, Maeike Zijlmans, George Petkov, Demetrios Velis, Steven Claus, Gergard Visser, Marcus Koppert, Fernando Lopes da Silva

Abstract—**High frequency oscillations (HFO) in stereo electroencephalographic (SEEG) signals have been recently the focus of attention as biomarkers that can have potential predictive power for the spatial location and possibly the timing of the onset of epileptic seizures. In this work we present a case study where we compare two quantitative paradigms for automated detection of biomarkers, one based on spontaneous SEEG recordings of HFOs and the other using activity induced by direct electrical stimulation (relative Phase Clustering Index algorithm). We compare the performance of these automated methods with manually detected HFO ripples by a trained EEG analyst and explore their potential diagnostic relevance. Intra-cranial recordings from patients undergoing pre-surgical evaluation are processed with a combination of morphological filtering and the analysis of the auto-correlation function. The results were compared to those obtained by visual inspection and to results from an active paradigm involving stimulation with 20 Hz trains of biphasic pulses. The quantity of HFOs, estimated automatically, or "rippleness", was found to correspond to the findings of a trained EEG analyst. The relative phase clustering index (rPCI) obtained using periodic stimulation appeared to be associated with the closeness to the seizure onset zone (SOZ) detected from ictal epochs. The HFO estimates were also indicative for the SOZ but with less specificity.**

I. Introduction

Epilepsy is a dynamic neurological condition where apparently normal states are intermittently disrupted by pathological states called seizures [1, 2]. Most patients considered for surgical treatment have to undergo lengthy observations, sometimes for several weeks, in order to determine the origin of epileptic seizures, or the location of the seizure onset zone (SOZ). In addition to scalp EEG recordings, invasive intracranial recordings (SEEG) may be required. To increase the efficiency and to reduce the length of the pre-surgical diagnostics, protocols based on active sub-clinical provocative electrical stimulation with various stimulation protocols and data analysis strategies were developed [3-5]. Another approach is based on the detection of spontaneous high frequency oscillations (HFO) generated from the neuronal tissue. HFO (ripples, fast ripples) are generally defined as oscillatory EEG components with frequencies in the range of 80-500Hz [6]. It is widely believed that their presence during the interictal periods can be indicative for the location of the SOZ [4, 7-11]. The mechanisms of HFO generation are a matter of current research [12]; their connection to the epileptic states has been proposed mainly based on recent animal models studies [13-15]. While in most cases the HFO detection has been based on visual inspection of filtered EEG traces [7] recently the automated detection of HFO has been addressed by increasing number of researchers [16-18] . Our contribution aims at a robust quantification of the HFO's in SEEG traces. The method we propose does not attempt to detect individual ripples in the signal but only to quantitatively assess their rate of occurrence. We do not use linear filtering since this may introduce spurious oscillatory components [16]. Our method is based on two novel techniques: (1) a modified Huang morphological signal decomposition [19-22] and (2) the computation of the autocorrelation function [23]. We compare the proposed method to the findings of visual inspection. In addition we compare the results with those obtained using the stimulation-based paradigm to compute the relative Phase Clustering Index as we introduced previously [5].

*Resrach supported in part by ZonMw agency in The Netherlands.

S.Kalitzin is with the Foundation Epilepsy Institute of The Netherlans (SEIN), Achterweg 5, 2103 SW, Heemstede, The Netherlands, (corresponding author, tel +31 235588248; e-mail: skalitzin@sein.nl).

Maeike Zijlmans (mzijlmans@sein.nl), George Petkov (gpetkov@sein.nl), Demetrios Velis (dvelis@sein.nl), Steven Claus (sclaus@sein.nl) Gergard Visser (gvisser@sein.nl), Marcus Koppert (mkoppert@sein.nl) are with SEIN.

Fernando Lopes da Silva is with Swammerdam Institute for Life Sciences, Faculty of Biology, University of Amsterdam, Amsterdam, The Netherlands and Department of Bioengineering, Instituto Superior Técnico, Lisbon Technical University, Lisbon, Portugal (e-mail: silava@science.uva.nl).

II. Patient Data and Signal Processing

A. Patient and data acquisition

The patient was recruited after informed consent to participate in this study. Scalp recordings EEG/CCTV failed to convincingly lateralize and/or localize the Seizure Onset Zone (SOZ); thus intracranial seizure recordings with depth electrodes (obliquely inserted with computer assisted navigation) were made in the Epilepsy Monitoring Unit (EMU) in our facility. The electrodes (Ad-Tech®, Racine, WI, USA) were implanted in the Free University Medical Centre Amsterdam. The implantation schemes were determined by a clinical neurophysiologist (DV and SC) according to previous diagnostic and clinical data. In Table 1 the relevant clinical information and the neurophysiologic findings are summarized.

The signals from the implanted contacts were digitized and recorded with a 65-channel Schwarzer® amplifier (Schwarzer GmBH, Germany) coupled to a workstation with Harmonie® 6.2 EEG acquisition (Stellate systems, Montreal, Canada) software. We used a sampling rate of

Table I. Patient Data

Patient, Seizures type	Imaging data	Contacts close to SOZ, first two most prominent in the 17 registered seizures
Female, 32 years old, PC	Evidence for left-sided mesial temporal sclerosis.	MTHCL 1,AHTCL 1, IAIL 2-4, AML 1-2, IAPL 1-4, TPL 1-3,

Table 1. Information about the pre-implantation anatomical (MRI) findings and neurophysiologic localization (visual inspection of peri-ictal SEEG done by board-certified neurophysiologists SC and DV). PC-partial complex.

1kHz, the hardware filters were: low-pass 300Hz, low-pass 0.016 Hz and no extra signal filtering was applied. All recordings were done using a referential montage. The identification of the contacts closest to the SOZ was done on basis of visual inspection of the ictal transitions in 17 registered seizures by a certified neurologist (SC).

B. Visual HFO detection

The visual detection of HFO or ripples was done by a trained neurophysiologist (MZ) who is experienced in segmenting ripples in large sets of SEEG data. Epochs of approximately 30sec artifact-free SEEG were selected; a high-pass linear FIR filter (80Hz) was used and the operator marked the beginning and duration of the ripples as events on the trace where the ripple was identified. All traces were considered independently and no multi-channel detections were made. Ripples shorter than 4 oscillation periods were discarded, also ripples closer than approximately two oscillatory periods were considered as one. To quantify the amount of HFOs in the visual detection, we estimated the total length of the detected ripples -T and the total amount of detected ripples - N for each individual SEEG trace.

C. Huang decomposition and filtering

We used the morphological decomposition of the signal known as Huang-Hilbert transform [19]. The method is based on decomposition of the signal into a hierarchy of components similar to those obtained from wavelet techniques but without using any pre-defined set of templates. If $S(t)$ is a SEEG trace in a finite time interval and sampled at certain frequency, then we denote as $\{M_a, t_a\}, a = 1 \ldots N_M$ and $\{m_\alpha, t_\alpha\}, \alpha = 1 \ldots N_m$ the sets of all local maxima and local minima correspondingly lying in the given time interval. From those two sets we use the cubic interpolation formula for the set of maxima, giving for each time point $t_a \le t < t_b$ the interpolated function

$$M(t) = M_a + (M_{a+1} - M_a)\frac{3(t_{a+1} - t_a)(t - t_a)^2 - 2(t - t_a)^3}{(t_{a+1} - t_a)^3} \quad (1)$$

Analogously for the minima we obtain an interpolated function $m(t)$. The next step is to define the decomposition "fast" and "slow" components

$$S(t) \equiv S_1(t) + R_1(t); R_1(t) \equiv \frac{M(t) + m(t)}{2} \quad (2)$$

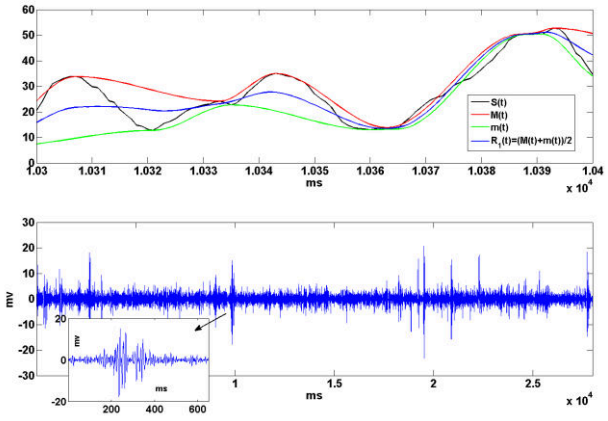

Figure 1. Illustration of a single step Huang transform. The upper plot shows the input signal (black trace) the interpolated curve over the local maxima (red trace), the interpolated curve over the local minima (green trace) and the average defined in equation (2) of the last two curves giving the slow component (blue trace). The bottom plot shows the filtered according to eq. (4) signal from one SEEG trace. The inset frame shows an individual ripple enlarged. The horizontal axes represent time in ms and the vertical the EEG measured signal in mV.

Decomposition (2) can be continued recursively, now using the residuals R(t) as input obtaining thus slower and slower components of the signal as:

$$R_k(t) \equiv S_{k+1}(t) + R_{k+1}(t), k = 1,2,... \quad (3)$$

In this way we obtain a multi-scale representation of the signal. The last decomposition can be defined for example as the step N when the slow component $R_N(t)$ has no more than a given number of local extrema. We selected this number to be zero defining the last scale as the DC or monotonic trend of the signal. Figure 1 shows an illustration of the Hung decomposition.

From the Huang decomposition we can define local frequency as $\omega_k(t) = 2\left(t_k^{a-1} - t_k^a\right)^{-1}$ where $\left\{t_k^a\right\}$ is the set of all local extrema of $S_k(t)$ and $t_k^{a-1} \le t < t_k^a$. This definition allows to perform band-pass filtering on the Huang decomposition of a signal as:

$$\Phi(S(t)) \equiv \sum_k S_k(t)\mu_k(t); \mu_k(t) = \begin{cases} 1, \omega_k(t) \in [\omega_{\min}, \omega_{\max}] \\ 0, \omega_k(t) \notin [\omega_{\min}, \omega_{\max}] \end{cases} \quad (4)$$

In the subsequent analysis we used high-pass filtering in the range above 80Hz, $[\omega_{\min}, \omega_{\max}] = [80, \inf]$.

D. Autocorrelation analysis

To extract what we call the "rippleness" of the signal we computed first the autocorrelation function

$$AC(\tau) = \langle S(t)S(t+\tau) \rangle_t \quad (5)$$

Using Hilbert transform we can obtain the analytical extension of (5) as

$$\overline{AC}(\tau) \equiv AC(\tau) + \frac{i}{\pi} p.v. \int_{-\infty}^{\infty} \frac{AC(\tau_1)}{\tau - \tau_1} d\tau_1 \quad (6)$$

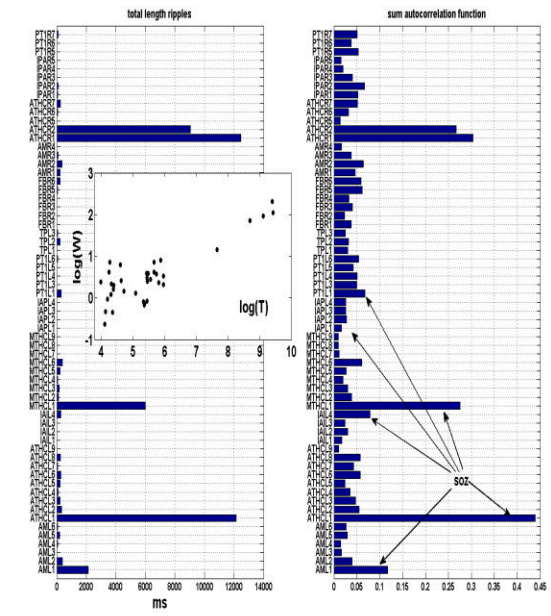

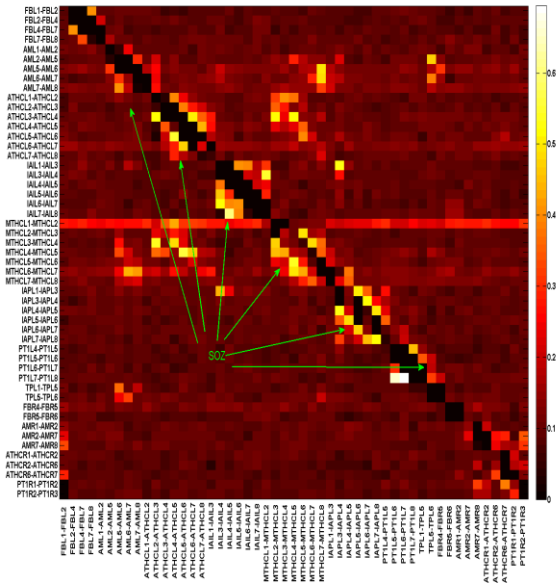

Figure2. ***Top frame.*** The left plot represents the total duration of epochs identified manually as HFO's (horizontal axis in ms) by the clinical expert for each channel (indicated along the vertical axis). The right plot shows the output of the computed quantity (7), the total power of ripples in the filtered signals. The arrows represent the contacts closest to the ictal onset zone during transitions to seizure. The inserted frame is the scattered plot between the logarithms of the manual (horizontal axis) an the automated (vertical axis) HFO quantifications. ***Bottom frame.*** The complete scan of the rPCI quantity. On the vertical axis are indicated the labels of the pairs of channels that were stimulated, typically all the neighboring contacts on each intracranial bundle. On the horizontal axis are the same channels-pairs in the same order where rPCI was measured using bipolar montages. High values of rPCI are indicated on a pseudo-color plot. Highest rPCI values for each stimulation pair is found at the neighboring contact pairs. The green arrows point to the contact groups on the main diagonal associated with the SOZ. Note that the stimulation of ATHCL contacts elicits large rPCI values on MTHCL contacts, and vice-versa. Stimulation at AML elicits rPCI at MTHCL sites but not vice versa. This indicates the existence of functional bi- or unidirectional connections between the local circuits.

The following quantity represents the estimation of the total power of HFO above 80Hz, or the "rippleness"

$$W \equiv \left\langle \left| \overline{AC}(\tau) \right| \right\rangle_{\tau>0} \tag{7}$$

E. *Relative phase clustering index (rPCI)*

Our stimulation based technique has been introduced and explained in detail previously [3, 5]. Here we recall that it is based on periodic, stimulation with a "carrier frequency" of 20Hz bi-phasic pulses, 0.5mA, cyclically alternating the polarities of each following stimulus (200 stimuli in total). Performing discrete Fourier transformation on the evoked response $R^{c,s}(t)$,(c-channel, s stimulus, f-frequency, t-time)

$$Z_f^{c,s} \equiv \frac{1}{\sqrt{N_t}} \sum_t e^{2\pi i f t} R^{c,s}(t) \tag{8}$$

We decompose the averaged evoked response complex amplitude as follows:

$$\langle Z_f^{c,s} \rangle_s = PCI^c{}_f \, \langle Z_f^{c,s} \rangle_s \equiv PCI_f^c A_f^c \tag{9}$$

To quantify the phase clustering of the harmonic components and to cancel the linear response effect we do a pair-wise response addition leading to the following definition for the phase clustering index, or the PCI.

$$PCI_f^c \equiv \left| \frac{< Z_f^{c,2s-1} + Z_f^{c,2s} >_s}{< | (Z_f^{c,2s-1} + Z_f^{c,2s}) | >_s} \right| \tag{10}$$

Finally we introduce the quantity the relative Phase Clustering Index, or rPCI, that is used in this work as a biomarker of "epileptogenic potential" as:

$$rPCI^c = \max_f \left(PCI_f^c \right) - PCI_1^c \tag{11}$$

III. Results

We present in figure 2, top frame, the results from the manual and automated detection of HFO showing the comparison of the two methods. We see from the inserted frame that the findings obtained by visual detection expressed in the total ripple length, essentially match those obtained from the automated detection provided by the quantity (7). This correspondence is not strictly monotonic and shows some scatter, especially for the channels of low HFO presence. To quantify the relation, we used the unidirectional non-linear association index h^2 measuring best functional fit between two measurement sets [24]. We found that $h^2(T,W) \approx 0.99; h^2(W,T) \approx 0.97; p < 0.01$ for the whole set of values measured on each electrode pair. The high value in both directions indicates the existence of a monotonic functional map between the manual and the automated "rippleness" estimates. The distribution of rPCI values obtained by stimulating the set of electrode pairs and measured from the same set is presented as a 2D pseudo-color intensity image on the bottom frame of figure 2. To explore the correspondence between the two (manual and automated) HFO and the rPCI measures to the clinically

relevant SOZ, we used the findings provided by certified neurologists (D.V. and S.C.) in Table I. Those findings were based on a visual peri-ictal SEEG observation. Accordingly, the bundles of arrows in the top and in the bottom frames represent the association of the HFO presence or the rPCI values with the closeness to the SOZ . We see that while relatively higher presence of HFO is visible, this criteria alone is not sufficient to identify the SOZ. HFO were present abundantly also in two traces at the right hippocampus (ATHCR1-2) in contrast to the rPCI measure which indicated high values only at those left implanted electrode bundles found as the closest to the SOZ (the green arrows on the bottom frame of figure 2). This corresponds more specifically to the ictal SOZ identification indicating seizures of exclusively left origin. We found no significant differences in the average length of the visually identified ripples among the EEG traces, all had an average length of approximately 100ms.

IV. Conclusions and discussion

The robust quantification of HFOs presence, the clinical relevance of HFOs for the condition of epilepsy and the mechanisms underlying HFOs generation (and possibly their causal relation to seizure onsets) are three major challenges in the research related to HFO. This study contributes to positively answering the first of the challenges and gives some hope for the second. Automated HFO detection has the advantage of high reproducibility and if proven the diagnostic value of HFO, the quantitative analysis can become a supplementary diagnostic tool for localization of the SOZ. Here we report also that methods using the active stimulation by means of which rPCI is estimated appear to have advantages compared to passive signal observation techniques.

V. References

[1] F. H. Lopes da Silva, W. Blanes, S. N. Kalitzin, J. Parra, P. Suffczynski, and D. N. Velis, "Dynamical diseases of brain systems: different routes to epileptic seizures," *IEEE Trans Biomed Eng,* vol. 50, pp. 540-8, May 2003.

[2] F. H. Lopes da Silva, W. Blanes, S. N. Kalitzin, J. Parra, P. Suffczynski, and D. N. Velis, "Dynamical diseases of brain systems: different routes to epileptic seizures," *IEEE transactions on bio-medical engineering,* vol. 50, pp. 540-548, 2003.

[3] S. Kalitzin, D. Velis, P. Suffczynski, J. Parra, and F. L. da Silva, "Electrical brain-stimulation paradigm for estimating the seizure onset site and the time to ictal transition in temporal lobe epilepsy," *Clin Neurophysiol,* vol. 116, pp. 718-28, Mar 2005.

[4] M. A. van 't Klooster, M. Zijlmans, F. S. Leijten, C. H. Ferrier, M. J. van Putten, and G. J. Huiskamp, "Time-frequency analysis of single pulse electrical stimulation to assist delineation of epileptogenic cortex," *Brain,* vol. 134, pp. 2855-66, Oct 2011.

[5] S. Kalitzin, J. Parra, D. N. Velis, and F. H. Lopes da Silva, "Enhancement of phase clustering in the EEG/MEG gamma frequency band anticipates transitions to paroxysmal epileptiform activity in epileptic patients with known visual sensitivity," *IEEE Trans Biomed Eng,* vol. 49, pp. 1279-86, Nov 2002.

[6] L. Andrade-Valenca, F. Mari, J. Jacobs, M. Zijlmans, A. Olivier, J. Gotman, and F. Dubeau, "Interictal high frequency oscillations (HFOs) in patients with focal epilepsy and normal MRI," *Clin Neurophysiol,* vol. 123, pp. 100-5, Jan 2011.

[7] L. P. Andrade-Valenca, F. Dubeau, F. Mari, R. Zelmann, and J. Gotman, "Interictal scalp fast oscillations as a marker of the seizure onset zone," *Neurology,* vol. 77, pp. 524-31, Aug 9 2011.

[8] P. N. Modur, S. Zhang, and T. W. Vitaz, "Ictal high-frequency oscillations in neocortical epilepsy: implications for seizure localization and surgical resection," *Epilepsia,* vol. 52, pp. 1792-801, Oct 2011.

[9] N. Usui, K. Terada, K. Baba, K. Matsuda, F. Nakamura, K. Usui, M. Yamaguchi, T. Tottori, S. Umeoka, S. Fujitani, A. Kondo, T. Mihara, and Y. Inoue, "Clinical significance of ictal high frequency oscillations in medial temporal lobe epilepsy," *Clin Neurophysiol,* vol. 122, pp. 1693-700, Sep 2011.

[10] M. Zijlmans, P. Jiruska, R. Zelmann, F. Leijten, J. G. R. Jefferys, and J. Gotman, "High frequency oscillations as a new biomarker in epilepsy," *Annals of Neurology,* pp. n/a-n/a, 2011.

[11] J. Jacobs, P. LeVan, R. Chander, J. Hall, F. Dubeau, and J. Gotman, "Interictal high-frequency oscillations (80-500 Hz) are an indicator of seizure onset areas independent of spikes in the human epileptic brain," *Epilepsia,* vol. 49, pp. 1893-907, Nov 2008.

[12] S. Demont-Guignard, P. Benquet, U. Gerber, A. Biraben, B. Martin, and F. Wendling, "Distinct hyperexcitability mechanisms underlie fast ripples and epileptic spikes," *Annals of Neurology,* pp. n/a-n/a, 2011.

[13] A. Bragin, J. Engel, Jr., C. L. Wilson, I. Fried, and G. W. Mathern, "Hippocampal and entorhinal cortex high-frequency oscillations (100--500 Hz) in human epileptic brain and in kainic acid--treated rats with chronic seizures," *Epilepsia,* vol. 40, pp. 127-37, Feb 1999.

[14] A. Bragin, C. L. Wilson, J. Almajano, I. Mody, and J. Engel, Jr., "High-frequency oscillations after status epilepticus: epileptogenesis and seizure genesis," *Epilepsia,* vol. 45, pp. 1017-23, Sep 2004.

[15] A. Bragin, C. L. Wilson, and J. Engel, "Spatial stability over time of brain areas generating fast ripples in the epileptic rat," *Epilepsia,* vol. 44, pp. 1233-7, Sep 2003.

[16] N. Jmail, M. Gavaret, F. Wendling, A. Kachouri, G. Hamadi, J. M. Badier, and C. G. Benar, "A comparison of methods for separation of transient and oscillatory signals in EEG," *J Neurosci Methods,* vol. 199, pp. 273-89, Aug 15 2011.

[17] R. Zelmann, F. Mari, J. Jacobs, M. Zijlmans, F. Dubeau, and J. Gotman, "A comparison between detectors of high frequency oscillations," *Clin Neurophysiol,* vol. 123, pp. 106-16, Jan 2012.

[18] N. von Ellenrieder, L. P. Andrade-Valenca, F. Dubeau, and J. Gotman, "Automatic detection of fast oscillations (40-200Hz) in scalp EEG recordings," *Clin Neurophysiol,* Sep 20 2011.

[19] N. Huang, Z. Shen, S. Long, M. Wu, H. Shin, Q. Zheng, N.-C. Yen, C. Tung, and H. Liu, " The empirical mode decomposition and Hilbert spectrum for nonlinear and non-stationary time series analysis. ," *Proceedings - Royal Society. Mathematical, physical and engineering sciences; ,* vol. 454, pp. 903-995., 1998.

[20] A. Pigorini, A. G. Casali, S. Casarotto, F. Ferrarelli, G. Baselli, M. Mariotti, M. Massimini, and M. Rosanova, "Time-frequency spectral analysis of TMS-evoked EEG oscillations by means of Hilbert-Huang transform," *J Neurosci Methods,* vol. 198, pp. 236-45, Jun 15 2011.

[21] R. J. Oweis and E. W. Abdulhay, "Seizure classification in EEG signals utilizing Hilbert-Huang transform," *Biomed Eng Online,* vol. 10, p. 38, 2011.

[22] H. Li, S. Kwong, L. Yang, D. Huang, and D. Xiao, "Hilbert-Huang transform for analysis of heart rate variability in cardiac health," *IEEE/ACM Trans Comput Biol Bioinform,* vol. 8, pp. 1557-67, Nov-Dec 2011.

[23] S. Kalitzin, M. Koppert, G. Petkov, D. Velis, and F. L. da Silva, "Computational model prospective on the observation of proictal states in epileptic neuronal systems," *Epilepsy Behav,* vol. 22 Suppl 1, pp. S102-9, Dec 2011.

[24] S. N. Kalitzin, J. Parra, D. N. Velis, and F. H. Lopes da Silva, "Quantification of unidirectional nonlinear associations between multidimensional signals," *IEEE Trans Biomed Eng,* vol. 54, pp. 454-61, Mar 2007.